Journal of Cleaner Production 379 (2022) 134595

Contents lists available at ScienceDirect

Journal of Cleaner Production

journal homepage: www.elsevier.com/locate/jclepro

# Feasibility of desalination by solar stills for small community scale freshwater demand

Sai Kiran Hota [a], Suryabhan Singh Hada [b], Catherine Keske [c], Gerardo Diaz [d,*]

[a] Advanced Cooling Technologies, Inc., Lancaster, PA, 17601, USA
[b] Department of Electrical Engineering and Computer Science, University of California, 5200 North Lake Rd., Merced, CA, 95343, USA
[c] Management of Complex Systems, University of California, 5200 North Lake Rd., Merced, CA, 95343, USA
[d] Department of Mechanical Engineering, University of California, 5200 North Lake Rd., Merced, CA, 95343, USA

ARTICLE INFO

Handling Editor: Mingzhou Jin

*Keywords:*
Solar stills
Solar desalination
Levelized cost of water
California
Rural communities

ABSTRACT

Solar stills are conventional desalination systems based on direct solar heating. While their productivity is limited, their simple construction and low maintenance requirements makes them an attractive and feasible option for community-scale desalination. This study shows that low-cost solar stills are capable of producing sufficient freshwater for small disadvantaged communities at costs lower than competing technologies. A variety of solar still materials are investigated showing that the cost of freshwater produced is sensitive to the solar still cost. Inexpensive carbon black particles dispersed in the water are used to increase solar still performance, and a set of low-cost solar still materials are identified from a pool of candidate materials to minimize water production cost by means of optical and energy analyses. In addition, communities with fewer than 10000 residents are identified in the reference region of California to perform an energy analysis to determine freshwater productivity yield and the cost of freshwater production. It is determined that a 10000 $m^2$ solar still could produce freshwater meeting the requirements of small rural communities costing less than $ 7.71 /$m^3$. Attractive investment options are available that could reduce the cost of water produced to less than $ 1.75 /$m^3$. Solar stills were found to be feasible when comparing the cost of freshwater produced with a comparable photovoltaic reverse osmosis system. The proposed methodology can be extrapolated to determine the feasibility of solar still-based desalination systems in other geographical locations. From the results of the analysis, solar stills are proposed for effectively producing low-cost freshwater to increase the accessibility of freshwater in small rural communities.

## 1. Introduction

Clean drinking water for human consumption is vital for subsistence. Several regions in the world currently facing severe water stress are in developing countries with significant rural population. Rural communities within developed nations like the United States (and specifically in certain areas of the State of California) also struggle with provisioning clean drinking water to rural communities and marginalized populations, due to high operating costs and complex logistics in low population density regions (Chappelle et al., 2022). To tackle the growing water crisis, renewable energy desalination plants such as membrane-based photovoltaic reverse osmosis (PV-RO), solar thermal/geothermal driven multi-stage flash, and multi-effect distillation are being investigated, installed and operated. These prominent technologies are not economically viable options for delivering low-volume freshwater (typically less than 200 $m^3$/day) to rural regions due to high capital costs and complex operational logistics associated with sparse populations. To meet rural scale freshwater demand, solar stills can be utilized. While PV-RO might be another feasible desalination system, this article demonstrates that solar stills are advantageous over PV-RO systems by significantly lowering capital, as well as operation and maintenance costs. The solar still collects energy passively, the materials are easily replaceable, and maintenance is affordable, which results in lower operational costs in comparison to PV-RO systems.

A solar still is comprised of a condensing cover, a basin and/or body with insulation, and a volume of saline water for desalination. A simple solar still design uses a single-slope condensing cover with a fixed tilt. Design improvements such as stepped solar still, internal mirrors, and integrating sun tracking were investigated by Abdallah et al. (2008). The use of all three design improvements resulted in

* Corresponding author.
*E-mail address:* gdiaz@ucmerced.edu (G. Diaz).

https://doi.org/10.1016/j.jclepro.2022.134595
Received 9 May 2022; Received in revised form 21 August 2022; Accepted 5 October 2022
Available online 7 October 2022

## Nomenclature

| | |
|---|---|
| $CAPEX$ | Capital cost, $ |
| $C_{pw}$ | Specific heat capacity of water, J/kg-K |
| $CT_{CO_2}$ | Carbon credits, $/ton-$CO_{2-eq}$ |
| $d'$ | Effective discount rate, % |
| $EE$ | Embodied energy, MJ |
| $EPBT$ | Energy payback time, year |
| $E_{out}$ | Energy produced in a year, MJ/year |
| $h$ | Heat transfer coefficient, W/m$^2$-K |
| $h$ | Heat transfer coefficient, W/m$^2$-K |
| $I$ | Solar irradiance, W/m$^2$ |
| $k$ | Thermal conductivity, W/m-K |
| $LCOW$ | Levelized cost of water, $/m$^3$ |
| $m_{annual}$ | Annual freshwater productivity, m$^3$/m$^2$-year |
| $m_w$ | Mass of water in basin, kg |
| $n$ | Refractive index |
| $Nu$ | Nusselt number |
| $OPEX$ | Annual Operation, maintenance, spares and replacement cost, $/y |
| $P$ | Saturation pressure, Pa |
| $PVF$ | Present worth function, year |
| $Q$ | Heat transfer rate, W |
| $R$ | Thermal resistance m$^2$ K/W$^{-1}$ |
| $Ra$ | Rayleigh number |
| $SV$ | Salvage value, $ |
| $T$ | Temperature, °C |
| $u$ | Wind velocity, m/s |
| $W_p$ | Peak power output, W |
| $z$ | Years of operation, year |

### Greek symbols

| | |
|---|---|
| $\alpha$ | Absorptivity |
| $\beta_{ext}$ | Extinction coefficient, m$^{-1}$ |
| $\delta_g$ | Thickness of glass, mm |
| $\epsilon_g$ | Emissivity of glass |
| $\kappa$ | Attenuation coefficient |
| $\lambda$ | Incident wavelength, nm |
| $\rho$ | Reflectivity |
| $\sigma$ | Stefan–Boltzmann constant, 5.68 × 10$^{-8}$ W/m$^2$-K$^4$ |
| $\tau_g$ | Transmissivity of glass |

### Subscripts

| | |
|---|---|
| $a$ | Ambient |
| $b$ | Basin |
| $ba$ | Coefficient between the basin bottom and the ambient |
| $cbw$ | Convection coefficient between the basin and basin water |
| $cga$ | Convection coefficient between the condensing cover and the ambient |
| $cwg$ | Convection coefficient between the basin water and the condensing cover |
| $ewg$ | Evaporation coefficient between the basin water and the condensing cover |
| $g$ | Condensing cover |
| $ins$ | Insulation |
| $rga$ | Radiation coefficient between the condensing cover and the ambient |
| $rwg$ | Radiation coefficient between the basin water and the condensing cover |
| $tba$ | Total coefficient between the basin and the ambient |
| $tga$ | Total coefficient between the condensing cover and the ambient |
| $twg$ | Total coefficient between the basin water and the glass |
| $w$ | Basin water |

### Abbreviations

| | |
|---|---|
| BOOT | Build, Own, Operate, Transfer model |
| EPA | Environmental Protection agency |
| MHI | Median household income |
| PV-RO | Photovoltaic reverse osmosis |

improving freshwater productivity by as much as 380%. Another design feature analyzed in the literature involved using fins in the solar still (Velmurugan et al., 2008). The freshwater productivity increased up to 45.5% with their design. Further design improvements included inverted, pyramid, spherical, hemispherical, and double-slope solar stills (Durkaieswaran and Murugavel, 2015). Another way of improving freshwater productivity involved the use of sensible energy storage materials, such as concrete, quartzite rocks, washed stones, or scrap iron (Murugavel et al., 2010), as well as phase change materials (PCMs) (Jahanpanah et al., 2021). Energy storage materials can help retain heat during heating cycles and discharge heat back to aid in desalination during the low-solar irradiation times like during sunset. Freshwater productivity improvements up to 30.9% were observed using PCMs (Jahanpanah et al., 2021). Traditional PCMs like paraffin wax are typically limited by poor heat transfer due to low thermal conductivity and non-uniform melt fraction, thereby, resulting in poor temperature distribution in the PCM (Guo et al., 2022c). Recently, PCM utilization has been shown to be improved by using horizontal fins (Yang et al., 2022), angled fins (Guo et al., 2022b), non-uniform angled fins (Guo et al., 2022c), non-uniformly distributed annular fins (Yang et al., 2020), and by the use of compressed metal foam saturated PCMs (Guo et al., 2022a). These features have shown significant improvement in achieving uniform and faster melting times and significant reduction average temperature difference in the PCM melt zone. These enhancements also improve the reliability of utilizing PCMs in solar stills. While freshwater yield improves significantly, these changes are capital intensive in comparison to the conventional design, especially having metal fins and solar trackers. An economical alternative is to use low-cost black carbon dispersion materials like activated carbon or biochar (Hota and Diaz, 2019, 2021). The advantage of using these dispersions is that the solar irradiation is absorbed closer to the evaporating surface rather than the black coated basin, where some energy is lost due to the buoyancy effects. The higher solar absorption at the evaporating surface increases the local water temperature which thereby, increases the solar still efficiency (Hota et al., 2022). These low-cost black carbon dispersion materials can enhance freshwater productivity rate by more than 60%, with a negligible increase in capital investment, thereby making solar stills more economically attractive over conventional systems (Hota et al., 2022).

Previous studies have found positive economic advantages of solar stills compared to PV-RO systems, but they have not addressed how advantageous material selection is to achieve low costs, as we do in our paper. Kalogirou (2005) noted that solar stills are economically advantageous systems that produce volumes of freshwater at a cost

lower than 200 $m^3$/day. Hota et al. (2022) noted solar stills to be favorable over solar collector integrated humidification–dehumidification and PV-RO systems for small scale freshwater production. Unlike PV-RO, solar still performance is less affected by salinity of feed water up to 8%, beyond which, the performance deteriorates by only 7% (Hoque et al., 2019). The possible reason is that the thermophysical properties of the water in the basin do not vary much for low salt concentrations.

A cost of freshwater for productivity in the range of 1 to 50 $m^3$/day was found to be between $4 to $24.7 per unit volume (1 $m^3$) of water (Madani and Zaki, 1995; Al-Hinai et al., 2002; Howe and Tleimat, 1974). To account for inflation, these costs are adjusted to 2021 USD corresponding to the reported values at the time of publication. However, there is little information on the feasibility of low-volume freshwater productivity (lower than 100 $m^3$/day) for solar stills.

The cost of freshwater produced from a solar still predominantly depends on the capital cost of the materials involved. One pertinent question, often asked in the literature, is how to find an appropriate combination of solar still materials for successfully operating such a system for economical freshwater production (Mathioulakis et al., 2007). This manuscript aims at identifying low-cost, durable, solar still materials to accomplish the eventual goal of producing and increasing accessibility of freshwater in small remote rural communities, especially in developing countries. A simple single basin solar still is considered for analysis in view of the increased complexity of stepped solar stills or solar still integrated with solar tracker (Dsilva Winfred Rufuss et al., 2018). The organization of the manuscript is as follows: firstly, low-cost, durable solar still materials with low embodied energy are identified from the literature based on the component requirements. Then, considering an inexpensive black carbon dispersion such as biochar (Hota and Diaz, 2021), the cost of freshwater produced for a given region is calculated by estimating the annual freshwater productivity rate and then applying the levelized cost of water (LCOW) method.

## 2. Methodology

In the present analysis, a single-slope, single-basin type solar still is considered. Potential solar still materials are identified based on the components requirements, to yield low-cost solar stills with low embodied energy. Then, for a chosen low-cost solar still system, the cost of desalination for the chosen reference location is calculated to determine the feasibility of utilizing a solar still system. The state of California was chosen as a reference location for two reasons: the state enjoys high annual solar energy potential, and it was identified as a persistent water stressed region a few years ago (MacDonald, 2007; Sengupta et al., 2018). Although an economically advanced region, there are several remote rural places with low-income small communities. The idea behind this analysis is to determine the potential of using a solar still system in disadvantaged-community locations.

For identifying suitable candidate materials, individual solar still component materials were investigated based on their requirements. A solar still essentially consists of a condensing cover, a basin to hold water, thermal insulation and the solar still body. The cover and the basin are separated by a certain distance and supported by the walls which form the body of the solar still. In this analysis, the condensing cover was considered to be fixed at a tilt angle of 37°, which is the average latitude of the reference region, to maximize the direct solar irradiation reaching the basin water. This dictates the height of the solar still and the volume of the solar still body. Sometimes, the solar still basin and the body are made up of the same material if its thermal conductivity is low, such as glass fiber reinforced plastic (GFRP). For each component, different materials are identified based on component requirements and compared based on their prices and the embodied energy to yield a 1 $m^2$ solar still. Then, a combination of low-cost materials is selected for the comparative economic analysis.

The economic analysis requires the calculation of freshwater productivity yield from the solar still system. This was done by making use of well-defined theoretical heat and mass balance equations. Real time solar irradiation, ambient temperature and wind velocity for the entire state of California were considered from the Cooperative Institute for Meteorological Satellite Studies (CMISS) public repository.[1] These data are derived from GOES-West satellite imagery using the Daytime Cloud Optical and Microphysical Properties Algorithm (DCOMP) (Walther and Heidinger, 2012). Then, for the chosen solar still system configuration, the cost of desalinating water is calculated. ($LCOW$) method, a concept similar to levelized cost of energy (or heat) was the methodology selected for the economic analysis. $LCOW$ is to account for system discounting across the system life. This is also compared to the cost of freshwater from the PV-RO system to ascertain solar still as a cost effective desalination system.

The schematic of the configuration is shown in Fig. 1. Along with the solar still, the system consists of overground water storage tanks for feeding saline water and freshwater. An underground storage tank, piping, and water pump are also part of the system. The reason for utilizing an underground storage tank is that the condensate is collected below the solar still due to gravity, so after obtaining a certain amount of freshwater, water can be pumped to an overground tank. The inherent assumption in the analysis is that the feed water source is either available nearby, or its transportation is already provided by the local administration.

## 3. Candidate solar still materials

The success of using solar stills lies in the fact that the component materials are low-cost and durable, provided they meet the component requirements. The common prerequisites for the components are: 1. Resistance to water corrosion and UV radiation; 2. Sustaining a temperature of at least 80 °C; 3. Sufficient strength to withstand ambient winds; and 4. Long shelf life. Additional component requirements for the condensing cover and the basin thermal insulation are mentioned below in Section 3.1.

### 3.1. Requirements for solar still components

#### 3.1.1. Condensing cover

The condensing cover is often made of a high transmitting material to make the solar still compact. For high transmissivity, the reflectivity and the absorptivity must be small. The cover reflectivity is a surface property and depends on the refractive index of the material. The reflectivity can be calculated by the formula

$$\rho_g = \left(\frac{n-1}{n+1}\right)^2 \tag{1}$$

where $n$ is the refractive index of the cover. Absorptivity of the condensing cover depends on the absorption coefficient ($\kappa$) and the thickness of the material ($\delta_g$). Absorptivity can be calculated as

$$\alpha_g = 1 - \exp\left(-\frac{4\pi\kappa}{\lambda}\delta_g\right) \tag{2}$$

The property $\frac{4\pi\kappa}{\lambda}$ is widely referred to as the extinction coefficient ($\beta_{ext}$) (Hota and Diaz, 2019; Modest and Mazumder, 2021). Typically, the cover thickness is about 3 to 4 mm. The transmissivity can be calculated as

$$\tau_g = 1 - \rho_g - \alpha_g \tag{3}$$

[1] See: ftp://ftp.ssec.wisc.edu/clavr/.

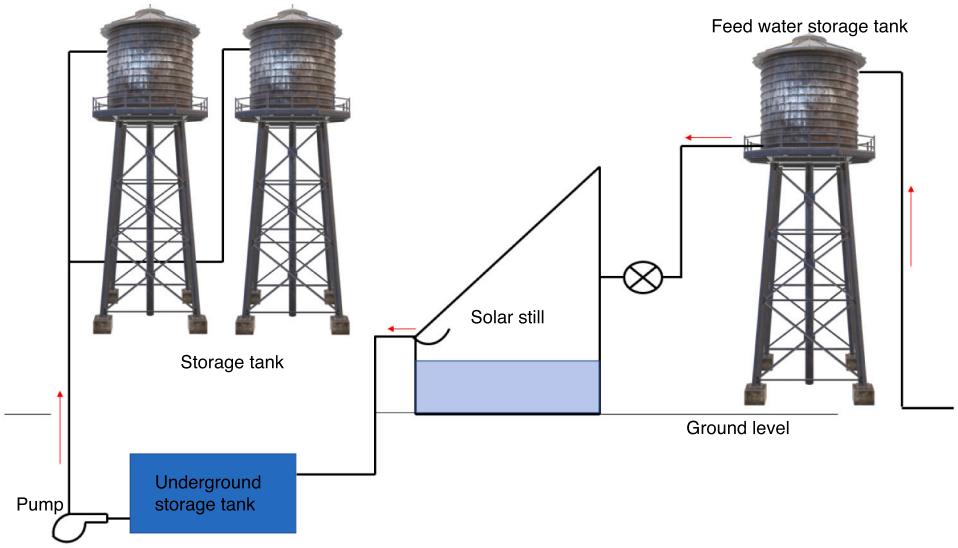


**Fig. 1.** Solar still desalination plant configuration.

### 3.1.2. Basin thermal resistance

The thermal losses from the basin of the solar still to the ambient must be minimized so as to have high freshwater productivity. It is estimated that freshwater productivity can be increased by at least 30% with good thermal insulation (Zheng, 2017). The basin and the thermal insulation form a series thermal resistance, which can be calculated as:

$$R_{bottom} = \frac{\delta_b}{k_b} + \frac{\delta_{ins}}{k_{ins}} \tag{4}$$

where, $\delta$ and $k$ are the thickness and thermal conductivity, and the subscripts $b$, and $ins$ correspond to the basin and thermal insulation, respectively. Usually, about 1 to 2 inches (approximately 2.5 to 5 cm) of insulation are utilized in the literature.

After determining a suitable insulation and basin material thickness, different material combinations were investigated from the literature and other sources based on the above mentioned constraints. To estimate low environmental foot print, energy payback time ($EPBT$) was used as a parameter, which is calculated as

$$EPBT = EE/E_{out} \tag{5}$$

where, $EE$ is the embodied energy and $E_{out}$ is the energy output in one year. $E_{out}$ is calculated by estimating freshwater productivity from the energy analysis as presented in Section 4 and multiplying it with the latent heat of water.

## 3.2. Candidate solar still materials

### 3.2.1. Condensing cover

For cover materials to be transparent with low reflectivity and absorptivity, the refractive index ($n$) should be less than 1.6, and the absorption coefficient ($\kappa$) must be below 0.0001. Glass materials tend to have values of optical indexes ($n$) less than 1.6, which results in reflectivity of 5%, and a weighted average solar absorptivity for absorption coefficient less than $10^{-6}$.

Fig. 2 shows the absorption coefficient for extinction coefficient values of 4 $m^{-1}$, 25 $m^{-1}$, and 32 $m^{-1}$ and glass materials that can be used as solar still cover materials. Typically, for different solar applications in use, the glass extinction coefficient is between 4 $m^{-1}$ to 32 $m^{-1}$ (Parkin, 2015). Soda lime glass, borosilicate glass, and silica glass meet the above mentioned optical index requirements. In this figure, the soda lime glass has a medium iron content (Vogt et al., 2016). Although some clear plastic materials such as polystyrene and polycarbonate can also be used, they are limited by their service temperature and service life (Ashby, 2011).

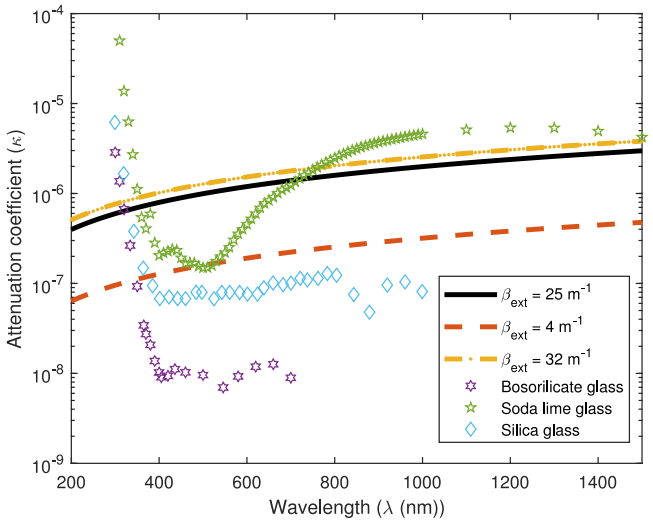


**Fig. 2.** Spectral absorption coefficient of candidate cover materials.

### 3.2.2. Basin thermal resistance

For determining the appropriate basin and insulation materials, firstly, the thermal resistance for optimal solar still performance was determined. The variation in solar still efficiency with bottom thermal resistance $R_{bottom}$, and the inter-dependency of the basin to obtain the optimal thermal resistance are shown in Fig. 3. The solar still efficiency is simply the ratio of net energy output in an hour to the incident solar energy in an hour.

### 3.2.3. Material choices

Suitable solar still component materials found in literature and analyzed here are mentioned in Table 1. The properties of the glass, basin, and sealant materials have been well documented by Ashby (2011). The properties of insulation materials were obtained from: EPS (Hill et al., 2018; Kumar et al., 2020), PS (Kecebas and Kayveci, 2010; Kunič, 2017), pUR (Braulio-Gonzalo and Bovea, 2017; Hill et al., 2018), GW (Kunič, 2017; Kumar et al., 2020), RW (Kecebas and Kayveci, 2010; Kunič, 2017), FG (Kecebas and Kayveci, 2010; Annibaldi et al., 2019), WF (Kunič, 2017; Annibaldi et al., 2019), SW (Schiavoni et al., 2016; Annibaldi et al., 2019), and cork (Kunič, 2017; Schiavoni et al., 2016).

**Table 1**
Selected solar still materials for analysis based on published literature.

| Cover (4 mm thick) | Basin (gauge 26) | Thermal insulation (R = 1.5 $m^2$ K $W^{-1}$) | Body | Sealant |
|---|---|---|---|---|
| Borosilicate glass | Stainless steel (SS) | Expanded polystyrene (EPS) | Concrete | Silicone epoxy (0.5 kg/$m^2$) |
| Soda lime glass | Galvanized steel (GS) | Extruded polystyrene (PS) | Granite | Glass putty (1 kg/$m^2$) |
| Silica glass | Brass | Polyurethane foam (pUF) | Sandstone | EPDM gasket (4 m/$m^2$) |
| – | Copper | Glass wool (GW) | Limestone | – |
| – | Granite (8 mm) | Rock wool (RW) | Wood | – |
| – | Sand stone (10 mm) | Fiber glass (FG) | GFRP | – |
| – | GFRP (4 mm) | Wood fiber (WF) | – | – |
| – | – | Sheep wool | – | – |
| – | – | Cork | – | – |

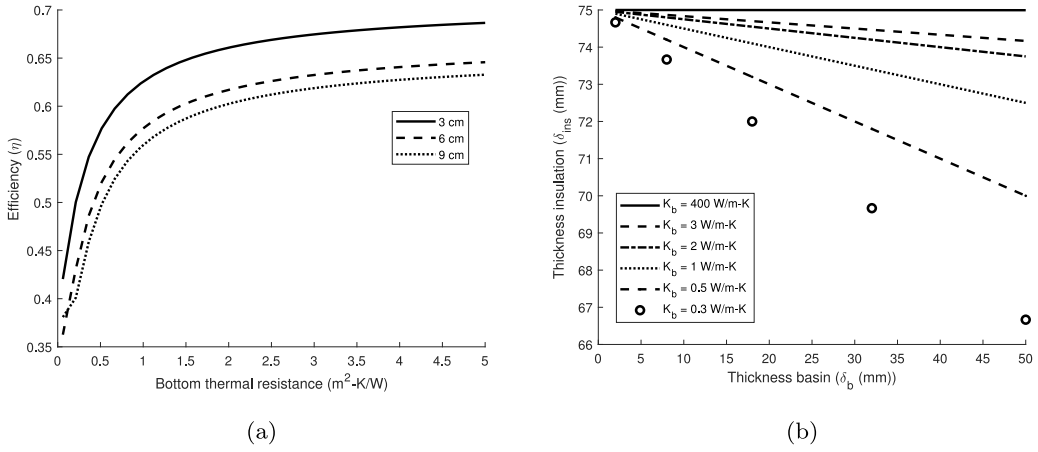


**Fig. 3.** (a) Variation of solar still performance with added heat resistance for 3 cm, 6 cm and 9 cm depths of basin water (R); (b) Thickness variation of the basin material and the insulation for a heat resistance (R) of 1.5 $m^2$ K $W^{-1}$.

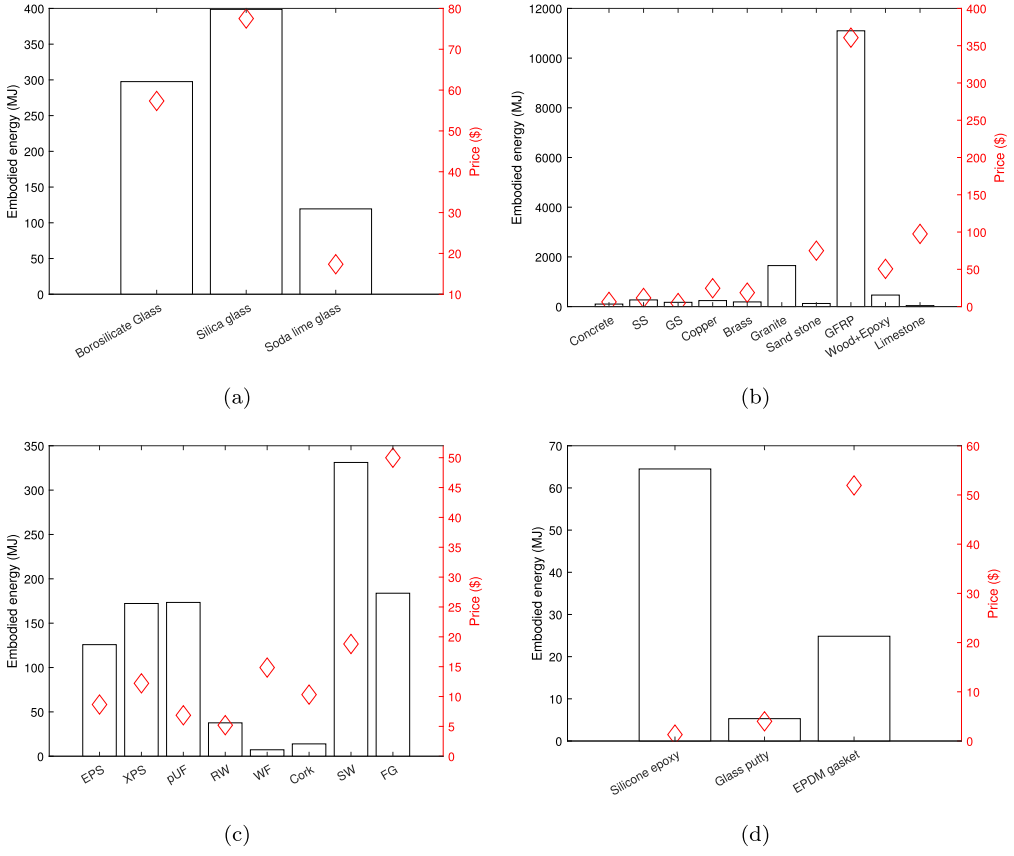


**Fig. 4.** Unit embodied energy and price of different candidate materials for (a) covers, (b) basin and body, (c) thermal insulation and (d) sealant.

**Table 2**
Resulting prices and $EPBT$ for different solar still material combinations.

| Cover | Basin | Thermal insulation | Body/frame | Sealant | Solar still cost ($/m$^2$) | $EPBT$ (years) |
|---|---|---|---|---|---|---|
| Soda lime glass | GS | RW | Concrete | Silicone | 32.55 | 0.25 |
| Soda lime glass | GS | pUR | Concrete | Silicone | 34.22 | 0.33 |
| Soda lime glass | GS | RW | Concrete | Putty | 35.25 | 0.25 |
| Soda lime glass | GS | EPS | Concrete | Silicone | 36.01 | 0.31 |
| Avoid combination below | | | | | | |
| Silica glass | Granite tile | Cork | Granite | Gasket | 731.16 | 1.11 |
| Borosilicate glass | Granite tile | FG | Granite | Gasket | 742.18 | 1.01 |
| Silica glass | Granite tile | FG | Granite | Gasket | 762.36 | 1.05 |

**Table 3**
Summary of candidate solar still materials requirements and recommended materials.

| Summary of requirements | | | | | |
|---|---|---|---|---|---|
| Common requirements | Withstand high temperatures<br>Withstand high wind loads<br>Resistant to water corrosion and UV radiation | | | | |
| Condensing cover | Basin/body & insulation | | | | Sealant |
| n < 1.6 | $R_{bottom} \geq 1.5$ m$^2$-K/W, non-porous | | | | Vapor leak tight |
| Recommended material | Cover | Basin | Thermal insulation | Body/frame | Sealant |
| | Soda lime glass | GS | RW | Concrete | Silicone |
| Limitations & Risk | Glass is brittle and must be carefully handled<br>Concrete wall is water permeable. GS sheet must cover the basin water depth<br>Sealant must be properly applied to make the solar still vapor leak tight | | | | |

Fig. 4 shows the price and the embodied energy of these solar component materials to produce a 1 m$^2$ solar still. A brief look at the charts shows that soda lime glass is the best option for glass, and GS sheet for the basin. Although concrete has low thermal conductivity and thereby has high thermal resistance to be used as the basin, it is water permeable and so it needs a non-porous sheet or coating over it. Interestingly, several researchers used GFRP as the basin, but it has a very high embodied energy and is an expensive material. More than 2500 combinations of solar stills were identified for these materials. Table 2 shows the suitable combination of materials for low-cost solar stills and their corresponding energy payback time.

It is seen that a 1 m$^2$ solar still can cost only around $32.5 with energy payback time of only 3 to 4 months. The last three rows show the material combinations that must be avoided, as 1 m$^2$ solar still costs much more than $700. Considering GFRP as the basin material, as was used in the literature, the cost of 1 m$^2$ solar still is around $450. This might be the reason for researchers having observed high cost of desalinated water in the respective solar stills with this material. The requirements of solar still component materials and potential low-cost choices are summarized in Table 3.

## 4. Energy analysis: Estimating freshwater productivity

### 4.1. Governing equations

An energy analysis was first performed to estimate annual freshwater productivity using mathematical models based on energy balances defined in the literature. The energy balance for different solar still components are as follows (Agarwal et al., 2017; Tiwari et al., 2003; Hota et al., 2022):

1. Glass cover:

$$\alpha_g' I + h_{twg}(T_w - T_g) = h_{tga}(T_g - T_a) \tag{6}$$

2. Basin:

$$\alpha_b' I = h_{cbw}(T_b - T_w) + h_{tba}(T_b - T_a) \tag{7}$$

3. Basin water:

$$m_w C_{pw} \frac{dT_w}{dt} = \alpha_w' I + h_{twg}(T_g - T_w) + h_{cbw}(T_b - T_w) \tag{8}$$

where, $I$, and $h$ represent incident hourly solar irradiation and the heat transfer coefficient. Subscripts $b$, $g$, $w$ and $a$ correspond to basin, glass, water, and ambient, respectively. Subscripts $c, r$, and $t$ correspond to convection, radiation, and total coefficients, respectively. Thus, $h_{twg}$ is total heat transfer coefficient between basin water and glass, $h_{tga}$ is total heat transfer coefficient between glass and the ambient, and $h_{tba}$ is the total heat transfer coefficient between the basin and the ambient. $h_{cbw}$ is the convective heat transfer coefficient between the basin and the basin water. The corresponding effective optical properties are given as follows (Agarwal et al., 2017; Elango et al., 2015):

$$\alpha_g' = \alpha_g(1 - \rho_g) \tag{9}$$

$$\alpha_w' = \alpha_w(1 - \alpha_g)(1 - \rho_g)(1 - \rho_w) \tag{10}$$

$$\alpha_b' = \alpha_b(1 - \alpha_w)(1 - \alpha_g)(1 - \rho_w)(1 - \rho_g)(1 - \rho_b) \tag{11}$$

The optical absorptivity for the materials is: 0.05 for glass; 1 for water; and 0.6 for the basin. The optical reflectivity for the materials is: 0.05 for glass; 0.05 for water; and 0.3 for the basin (Hota et al., 2022). The above equations are solved iteratively in MATLAB until the solution parameters converge to a residual tolerance of less than $10^{-4}$ to determine the hourly freshwater productivity, which is calculated as (Hota et al., 2022):

$$m_{hour} = \frac{h_{ewg}(T_w - T_g)}{I * A} \times 3600 \tag{12}$$

From the above Eq. (12), annual freshwater productivity is calculated by summing the hourly freshwater productivity through the year and multiplying with available plant factor of 96% considering 4% of downtime for maintenance (Hota et al., 2022).

The inherent assumptions involved in defining the above equations are as follows (Tiwari et al., 2003; Hota et al., 2022):

1. The heat capacity of the glass and the basin are negligible in comparison to water. Heat losses from the side walls are negligible.
2. The basin water temperature is uniform throughout the depth without stratification.
3. The envisioned solar still constructed is vapor leak tight.

### 4.2. Heat transfer coefficients

#### 4.2.1. Water to glass cover

The heat transfer coefficient $h_{twg}$ is the sum of the convective ($h_{cwg}$), radiative ($h_{rwg}$), and evaporation heat transfer coefficient ($h_{ewg}$) between the basin water and the condensing glass cover as (Hota et al., 2022):

$$h_{twg} = h_{cwg} + h_{rwg} + h_{ewg} \tag{13}$$

The convective heat transfer coefficient between the basin water and the condensing cover is given as (Dunkle, 1961):

$$h_{cwg} = 0.884\left[(T_w - T_g) + \frac{(P_w - P_g)(T_w(K))}{268900 - P_w}\right]^{1/3} \tag{14}$$

where, $P_w, P_g$ are saturation vapor pressures at basin water and glass cover temperatures.

The evaporative heat transfer coefficient is also given as a function of vapor pressure difference and temperature difference between the basin water and condensing cover as: (Dunkle, 1961; Cooper, 1973):

$$h_{ewg} = 0.0163 h_{cwg}\frac{P_w - P_g}{T_w - T_g} \tag{15}$$

The radiation heat transfer coefficient between basin water and the glass cover is calculated as (Agarwal et al., 2017):

$$h_{rwg} = 0.96\sigma(T_w(K)^2 + T_g(K)^2)(T_w(K) - T_g(K)) \tag{16}$$

#### 4.2.2. Bottom heat loss coefficient

The heat transfer coefficient between the basin water and the basin is given as (Hota et al., 2022):

$$h_{cbw} = \frac{Nuk_w}{L_c} \tag{17}$$

where, $k_w$ and $L_c$ are the thermal conductivity of the basin water and the characteristic length.

The Nusselt number is calculated as (Bergman et al., 2011; Zoori et al., 2013):

$$Nu = CRa_l^y \tag{18}$$

where, $C, y$ are 0.54, 1/4 if $10^4 \le Ra_l \le 10^7$; 0.15, 1/3 if $10^7 \le Ra_l \le 10^{11}$; or 0.52, 0.2 otherwise (Bergman et al., 2011).

The heat transfer coefficient from the basin to the ambient is a result of heat loss through conduction from the basin, insulation, and the ambient heat loss as (Agarwal et al., 2017; Hota et al., 2022):

$$h_{cba} = \left[R_{bottom} + \frac{1}{h_{ba}}\right]^{-1} \tag{19}$$

where, $h_{ba} = 5.7 + 3u$ (Lawrence et al., 1988).

#### 4.2.3. Top heat loss coefficient

The total top heat loss coefficient from the condensing cover to the ambient ($h_{tga}$) is the summation of the ambient convective ($h_{cga}$) and radiative heat loss coefficient ($h_{cga}$) from glass cover to the ambient which are given as (Hota et al., 2020):

$$h_{cga} = 2.8 + 3u \tag{20}$$

$$h_{rga} = \epsilon_g\sigma(T_g(K)^2 + T_{sky}^2)(T_g(K) + T_{sky}) \tag{21}$$

where, $T_{sky} = 0.0552T_a(K)^{0.5}$ (Hota et al., 2018).

Solving the above governing equations: Eqs. (6), (7), and (8) together results a first order transient differential equation with solution of the form (Tiwari et al., 2003; Hota et al., 2022):

$$T_w = \frac{\bar{f}(t)}{at}(1 - \exp(-at \times t)) + T_{w0}\exp(-at \times t) \tag{22}$$

where, $t$ is computational time, $at$ is thermal time constant, $T_{w0}$ is the initial basin water temperature; and $f$ is a function of effective light absorptivity, and heat loss coefficient. After determining the basin water temperature, the basin and condensing temperatures are calculated as:

$$T_g = \frac{\alpha_g' I + h_{twg}T_w + h_{tga}T_a}{h_{twg} + h_{tga}} \tag{23}$$

$$T_b = \frac{\alpha_b' I + h_{cbw}T_w + h_{tba}T_a}{h_{cbw} + h_{tba}} \tag{24}$$

### 4.3. Results: Estimated freshwater productivity

#### 4.3.1. Model validation

The thermal model for single-slope solar still was validated against experimental data published in the literature (Agarwal et al., 2017). The experiments were performed with a single slope solar still with varying feed water depths of 2 cm, 4 cm, 6 cm, 8 cm, and 10 cm. The solar still was made with galvanized steel of dimensions 0.85 m × 0.6 m × 0.2 m and was placed inside a box consisting of plywood and polystyrene insulation. The basin of the solar still was painted black. The average hourly basin water temperature and cumulative freshwater productivity rate predicted by the thermal model and the experimental data now follows.

Fig. 5 shows the comparison of the basin water temperature and the cumulative freshwater productivity predicted by the thermal model and the published experimental results for varying basin water depths. As the basin water depth increases, the maximum achievable temperature decreases and shifts towards the afternoon hours instead of the time when the solar irradiation is the highest. This happens due to higher thermal inertia of the deeper basin water compared to the shallow basin water. Although the maximum temperature of the deeper basin water is lower, higher thermal inertia helps with decreased rate of temperature drop in the evening. Freshwater is still produced for some time even after the sunset. Overall, a good agreement between the thermal model and the experimental data was achieved.

#### 4.3.2. Freshwater productivity rate

The freshwater productivity rate is calculated to determine the annual freshwater production in the reference location. This is then used as the normalizing parameter for the cost of desalinated water.

Fig. 6 shows the estimated annual freshwater productivity rate with a 1 $m^2$ solar still at different locations in California at 96% plant availability. The freshwater productivity is expected to be almost uniform from a low value of 974.1 L/$m^2$-year to a maximum of 1080.3 L/$m^2$-year. The median distillate productivity rate is 1012.5 L/$m^2$-year. The freshwater productivity rate map shown in Fig. 6 does not directly reflect the daily average solar irradiation rate. While solar irradiation strongly influences the freshwater productivity, the ambient temperature and wind velocity also influence the freshwater productivity rate. For example, in the southern regions of California, where the solar irradiation is comparatively higher than in other parts of the state, the lower wind velocity does not contribute to lowering the cover temperature, which is important for high freshwater production rate. Likewise, the same inference can be drawn from the mountainous region (Eastern side) of the state. High surface heat losses from the cover increases the temperature difference between the evaporating pool and the condensing cover, thereby increasing productivity. It is seen that the maximum difference in freshwater production rate estimated for the state is only 106.2 L/$m^2$-year.

A parametric analysis was performed using the governing equations, i.e., Eqs. (6), (7), and (8), in MATLAB by changing one parameter at a time while other parameters were kept constant at the baseline value. Fig. 7 shows the parametric influence of varying various operating conditions on freshwater productivity rate. The chosen base values are: 5% cover absorptivity, 3.5% salinity, 6 cm insulation thickness, 4 cm saline water depth. High cover absorptivity and reflectivity and low thermal insulation thickness have adverse effects on freshwater

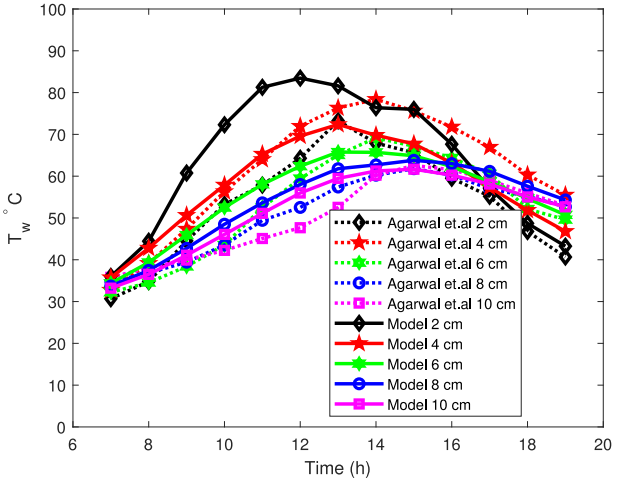


(a)

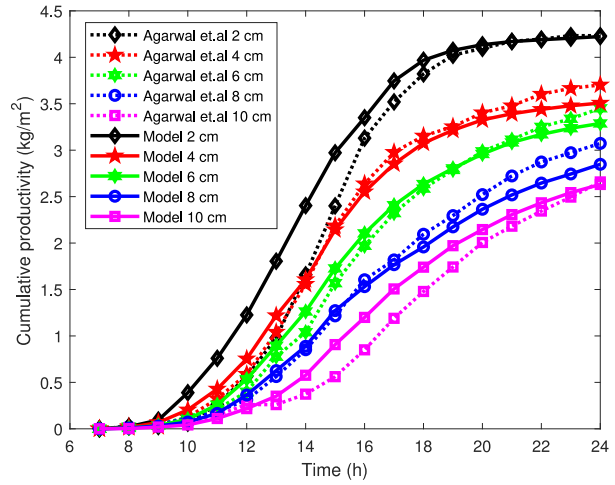


(b)

**Fig. 5.** Comparison of (a) Hourly basin water temperature, and (b) cumulative freshwater productivity between the experimental data and the thermal model.

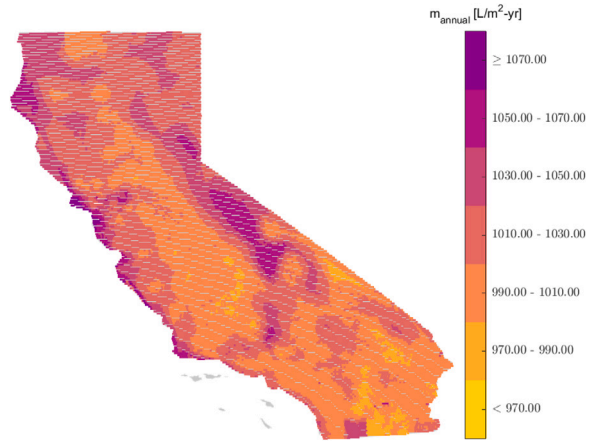


**Fig. 6.** Estimated annual freshwater productivity of solar still in the state of California.

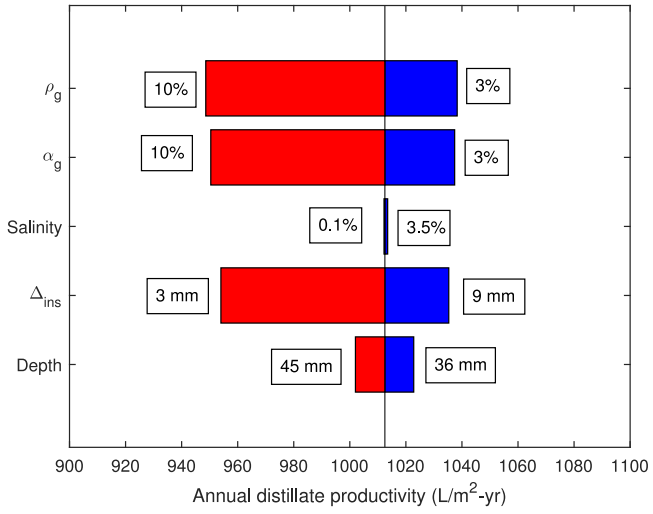


**Fig. 7.** Parametric influence of parameters affecting distillate productivity.

productivity. But at high optical values around 10% instead of 5%, freshwater productivity decreases by only 6% to around 954 L/m$^2$-year. The influence of varying the depth and salinity have less effect on freshwater productivity for the values considered.

## 5. Economic analysis

### 5.1. Cost considerations

Once the low-cost solar still materials were identified, an economic analysis was performed and the results were normalized for an output of 1 m$^3$ of freshwater produced. The costs of the solar still system can be divided into capital cost ($CAPEX$) and operational cost ($OPEX$). The capital cost of some of these materials vary with the land area (in terms of \$/m$^2$), while for the tanks or excavation, the cost varies with the volume. For such cost parameters, a correlation based on annual fresh water production rate ($m_{annual}$) was developed based on the prices found from a variety of sources. These capital investment items are shown in the Table 4. Indirect capital costs are taken as 30% of direct capital cost to account for system planning and design, engineering, contingency and insurance (El-Dessouky and Ettouney, 2002). One of the inherent assumptions is that the land for installing the system is available for free based on the Build, Own, Operate and Transfer (BOOT) model (El-Dessouky and Ettouney, 2002). The operations and maintenance cost are assumed to be 1.5% of the $CAPEX$, and the labor cost is expected to be size dependent between \$ 0.1/m$^2$ to \$ 0.6/m$^2$ (Thomas, 1997). A value of \$ 0.5/m$^2$ was considered. In addition, some of the common assumptions involved are: 1. A solar still operates for at least 25 years; 2. Sealant and pumps are expected to be replaced every 5 and 10 years, respectively; and 3. A 15% salvage value is assumed for the system components.[2]

The levelized cost of desalinated water from the solar still system is calculated as (Masters, 2013):

$$LCOW = \frac{CAPEX + (OPEX - CT_{CO_2}) * PVF - \frac{SV}{(1+d')^z}}{m_{annual} * PVF} \quad (25)$$

where $CT_{CO_2}$ is the carbon credits that are availed by the system. In the baseline scenario, $CT_{CO_2}$ is taken as zero. $PVF$ is the present worth function that accounts for the system discount rate and the future value of the annual investments (Masters, 2013).

The above formulation yields the cost of desalination. For the actual water supply, other cost items such as pre-treatment and post-treatment costs, and concentrate or salt disposal costs are also included. The cost

[2] See: https://iscrapapp.com/prices/ ; https://rockawayrecycling.com/scrap-metal-prices/.

**Table 4**
System cost for solar still desalination plant for the chosen configuration.

| Cost element | Cost | Comments | Reference |
|---|---|---|---|
| Saline feed pump | $ 750 | 72 $m^3$/h pumping rate, 1 year warranty | SAER-USA (2020a) |
| Fresh water pump | $ 150 | 3.6 $m^3$/h pumping rate, 1 year warranty | SAER-USA (2020b) |
| Feed storage tank | $ 1610.1 $* m_{annual}^{0.6373}$ | Power law as function of volume > 50 $m^3$ (Meratizaman et al., 2015) | State of Michigan (2003) |
| Distillate storage tank | $ 1680.8 $* m_{annual}^{0.6085}$ | Power law as function of volume < 50 $m^3$ (Meratizaman et al., 2015) | State of Michigan (2003) |
| Underground storage tank | $ 411.78 $* m_{annual}^{0.8693}$ | Power law as function of volume (Meratizaman et al., 2015) | National tank outlet (2003) |
| Excavation | $ 646.33 $* m_{annual}^{0.624}$ | Power law as function of volume (Meratizaman et al., 2015) | homewyse (2020) |
| Piping | $ 1500 | $ 1.5/ foot for CPVC pipe | United States Plastic Corp (2020) |

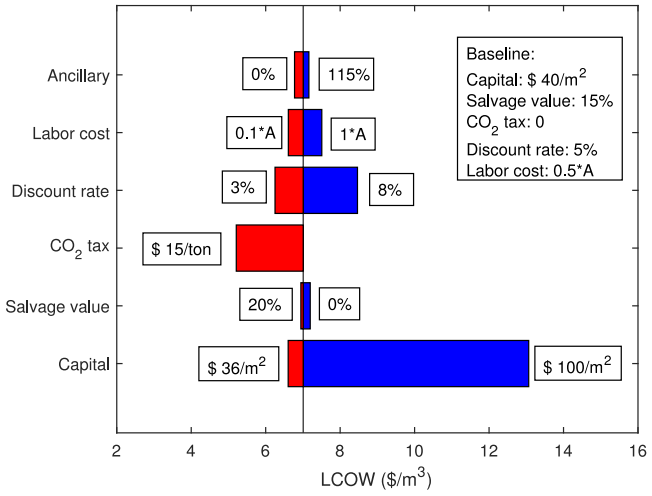


**Fig. 8.** Sensitivity analysis of cost components on $LCOW$.

estimates for these processes vary with desalination technology and size of the plant, where reliable information for the case of solar stills is not available. However, a simple estimation for treatment cost as used by Al-Hinai et al. (2002) could be 10% of capital cost. Ziolkowska and Reyes noted that the cost of brine disposal to a nearby water source could be between $0.33 and 0.66/$m^3$ (Ziolkowska and Reyes, 2017). These cost items can be added to the cost of desalination to determine the final cost of water supplied.

### 5.2. Cost of desalination

The cost of components in the numerator and the annual freshwater productivity rate used as the normalizing parameter in the denominator of the Eq. (25) changes with the area. The cost of the solar still was considered to be $40/$m^2$ including the low-cost carbon dispersions. A slightly higher value is considered here to account for variation in cost with time. The cost of inexpensive biochar dispersion with 0.1% volume concentration for full solar absorption is less than $0.1 for 1 $m^2$ basin area (Hota et al., 2022). Solar still systems varying from 10 $m^2$ solar still to 10,000 $m^2$ solar still were considered to analyze the influence of area. It was observed, as shown in Fig. S1, that the $LCOW$ decreases from a range [$ 49.1/$m^3$, 59.5/$m^3$] of freshwater produced for 10 $m^2$ solar still area to less than [$ 6.36/$m^3$, $7.71/$m^3$] for a 10,000 $m^2$ solar still. The lower and higher values reported are for annual freshwater productivity of 1100 L/$m^2$-year and 900 L/$m^2$-year, respectively. As seen from Eq. (25), the $LCOW$ curves flatten around the solar still basin area above 1000 $m^2$, which must be considered a minimum value for economically attractive solar still system installation. In this analysis, the solar still basin area considered was 10,000 $m^2$, where the median $LCOW$ for the state of California is $ 6.89/$m^3$.

Another solar still system configuration was considered assuming the solar still was installed above the ground. The 10,000 $m^2$ solar still mass (including basin water) of ≈ 600 tons must be supported by the pillars. The cost of concrete footing is about $10,000 for 4 pillars (HomeAdvisor, 2022). In addition, installing the solar still above the ground increases the labor maintenance costs. The estimated median $LCOW$ was $8.73/$m^3$ for this case. In this scenario, the capital cost associated with excavation, underground tank and pump in the original scenario is replaced by the cost of concrete support pillars and the increase in labor and maintenance cost, resulting in an increase in the $LCOW$. Also, the system installation cost, insurance costs, and other overhead $CAPEX$ and $OPEX$ will likely increase considering the risk associated with over the ground installation. The cost of water is extremely dependent on the capital cost of the system. In addition, the cost of desalination is also sensitive to some other parameters. A parametric sensitivity study was performed to understand the influence of different cost parameters.

The baseline value of $6.89 /$m^3$ shown in Fig. 8 is the median value of the baseline case. Detailed information on the cost distribution for the entire state will be shown below. The cost components that could influence the $LCOW$ are the solar still cost, costs of system components (ancillary), labor cost, discount rate, $CO_2$ tax credit, and salvage value. The corresponding values for the baseline case are mentioned in the text box of Fig. 8. A poor choice of solar still materials results in solar still cost of $100/$m^2$ and the $LCOW$ almost doubles to $13.06/$m^3$. Interestingly, the discount rate shows a relevant influence on the $LCOW$. At a lower feasible value of 3% (good investment), the $LCOW$ is $6.25/$m^3$, while for a larger value of 8% (bad investment), the $LCOW$ is $8.47/$m^3$. Availing carbon credits at a feasible value of $15/ ton of $CO_{2-eq}$ emissions results in a reduction of $LCOW$ to a value of $5.21/$m^3$. The other parameters have small influences on the cost of desalination.

Figure S2 shows the cost distribution for freshwater productivity with a 10 000 $m^2$ solar still for the selected configuration. In the baseline (normal) scenario, the $LCOW$ varies between $6.47/$m^3$ to $7.14/$m^3$ of freshwater produced with a median of $6.89/$m^3$. The lowest value is seen in regions where the freshwater productivity is high. However, the costs are almost uniform with a variation of only $0.67/$m^3$ since the freshwater productivity rates are almost the same. In the best (optimistic) case scenario, the $LCOW$ varies between $1.58/$m^3$ and 1.74 /$m^3$ with a median value of $1.68/$m^3$.

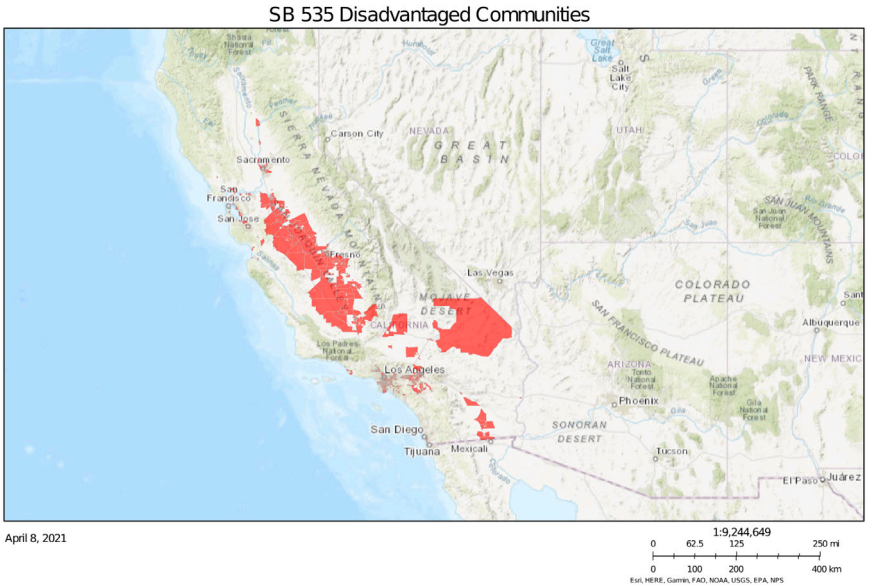


**Fig. 9.** Map distribution of disadvantaged communities in California.
*Source:* https://oehha.ca.gov/calenviroscreen/sb535.

### *5.3. Feasibility of solar still system in rural communities in chosen reference location*

While the chosen reference location is reasonably well developed, there are several counties (regions) in California whose reported mean household income (MHI) is lower than the state average of $75,235 (Chappelle et al., 2022; Census Reporter, 2019), where, the unit cost of freshwater must be preferably lower than $ 2.6/m$^3$ for one percent MHI allocation (Achari et al., 2018). With the best case scenario, the $LCOW$ is significantly lower than this value. If 10% of total capital cost is added as water treatment cost, and $ 0.5/m$^3$ as brine disposal cost (Ziolkowska and Reyes, 2017), then the median cost of water increases to $2.51/m$^3$ (increase by $0.83/m$^3$) in the best case scenario.

The map shown in Fig. 9 shows the distribution of low-income communities in the region. There are several regions in the state where the income levels are below the state average. If 5 liters of water is assumed per person (for drinking and cooking activities), 30 m$^3$ of freshwater production per day can serve a population of 6000 people. The MHI allocation for freshwater for 20 low-income regions of the state is shown in Table 5 for normal (baseline) investment and the best case investment scenarios. For the baseline case, the MHI allocation for the cost of water is expected to be between 3.8% and 9.2% with an average value of 6%. This results in a value higher than the MHI water affordability of 4.5% (Mack and Wrase, 2017). However, with the best case scenario investment, the MHI allocation for freshwater is between 1% and 2.3% at an average of 1.5%. This is below the EPA recommended maximum of 2.5% of national average MHI for communities smaller than 10,000 residents (Jones and Moulton, 2016).

**Table 5**
MHI allocation for freshwater in communities with fewer than 10 000 residents (U.S. Census Buraeu, 2019; Census Reporter, 2019). Average state MHI is $ 75 235.

| Location | Population | MHI ($) | MHI allocation: baseline (%) | MHI allocation: best case (%) |
|---|---|---|---|---|
| Chico | 4169 | 53 324 | 4.32 | 1.10 |
| Marysville | 2143 | 44 839 | 5.11 | 1.30 |
| Lodi | 4230 | 54 338 | 3.88 | 0.99 |
| Snelling | 2328 | 48 889 | 4.7 | 1.20 |
| Firebaugh | 1152 | 3516 | 6.53 | 1.67 |
| Mendota | 6562 | 31 237 | 7.37 | 1.88 |
| Laton | 3548 | 30 743 | 7.50 | 1.92 |
| Huron | 5569 | 25 060 | 9.19 | 2.35 |
| Lindsay | 3395 | 31 489 | 7.39 | 1.89 |
| Lost Hills | 3937 | 35 188 | 6.58 | 1.67 |
| Mc Kittrick | 5248 | 38 750 | 5.97 | 1.52 |
| Wofford Heights | 6158 | 29 718 | 7.60 | 1.94 |
| Arvin | 6401 | 38 464 | 6.05 | 1.55 |
| Taft | 6156 | 45 195 | 5.08 | 1.30 |
| Lancaster | 4514 | 55 237 | 4.14 | 1.06 |
| Baker | 3846 | 27 308 | 8.48 | 2.15 |
| Blythe | 3341 | 45 385 | 5.13 | 1.31 |
| Calipatria | 5007 | 36 883 | 6.30 | 1.62 |
| Westmorland | 2640 | 60 471 | 3.83 | 0.98 |
| Average | – | 40 744 | 6.03 | 1.54 |

## 6. Comparison to competing PV-RO system

In the preceding section, the median cost of freshwater productivity using a solar still is $6.89/m$^3$, with a value of only $1.68/m$^3$ in the best case scenario. The feasibility of desalination with a solar still is determined by comparing against the widely utilized PV-RO system for a similar range of freshwater productivities. The PV-RO system configuration requires a PV system, RO membrane and a storage tank for freshwater. The analysis for the region was performed by solving the mass balance equations on the RO membrane, where the PV system increases the pressure of saline water. The equations are shown in Table S1. Freshwater is only produced if the feed water pressure upstream of the RO membrane satisfies freshwater quality lower than 500 ppm (Water Systems Council, 2007). For the PV-RO economic analysis, the cost components are as follows: PV system cost: 2.25 $/W (Feldman and Margolis, 2020); RO membrane: $1000; Cost of pump function of hourly feed rate, $Q_{f,h}$, and feed pressure of 55 bar (Malek et al., 1996): $HPP = 52(Q_{f,h}P_f)$; Indirect cost: 30% of total direct capital cost (El-Dessouky and Ettouney, 2002); membrane replacement rate: 5 years; pump replacement rate: 10 years; labor cost as per contract wage law basis: $ 25 000/ year; annual operations and insurance cost: 1.5% total capital cost. A 100 m$^2$ PV system was considered to be sufficient for producing same volume of fresh water as that of the solar still analysis. The freshwater quality and assessment is mentioned below in Table 6.

Figure S3 shows the estimated annual freshwater (permeate) productivity in the state of California and its corresponding cost. Annual freshwater productivity rate has a wide range from 578.53 and 1739.7 L/m$^2$-year with a median productivity of 1264.3 L/m$^2$-year. The reason is that the freshwater yield only happens after the RO membrane

**Table 6**
Freshwater quality assessment.

| | Solar still | PV-RO |
|---|---|---|
| Quality | 0 ppm.<br>13 to 230 ppm from literature (Alwan et al., 2021) | ≤ 500 ppm |
| Influencing factor | Water is evaporated | RO upstream feed water pressure |

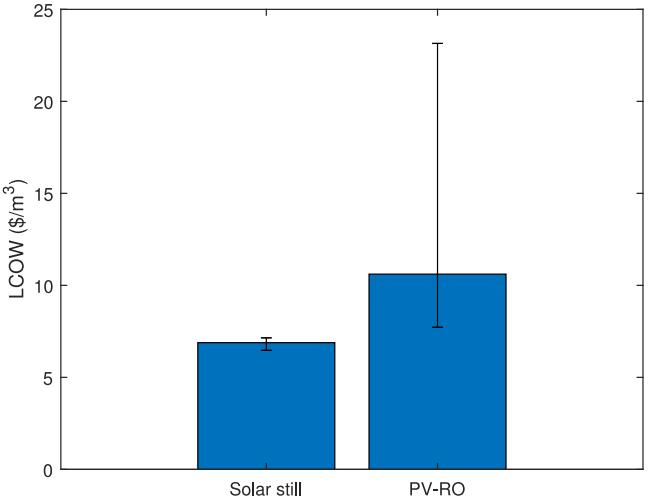


**Fig. 10.** Comparison of cost of water between solar still and PVRO.

reaches a minimum threshold of 40 bar. So at lower solar irradiation conditions, freshwater is not produced. The region of northern California is found to have very low productivity, but high freshwater productivity can be obtained in the southern California region. The distribution map is similar to the solar irradiation map of the region. Based on this productivity, the estimated $LCOW$ for the PV-RO technology is between $\$7.7/m^3$ and $23.1/m^3$ with a median value of $\$10.6/m^3$.

The cost of water produced from the solar still and PV-RO on a comparison basis is shown in Fig. 10. The cost of water produced with the solar still at $\$6.89/m^3$ is significantly lower than the PV-RO at $\$10.6/m^3$. As explained above, solar stills are more economical because of lower capital and operational costs. Also, $LCOW$ variation is small in the case of solar still compared to PV-RO because of a more uniform freshwater yield with solar still than with PV-RO.

From the analysis presented above, it was determined that solar still systems made of low-cost materials can produce freshwater at costs lower than the competing PV-RO technology for small community scale desalination due to the low capital cost of the system, and significantly lower operation and maintenance costs. This will have notable impact in improving freshwater accessibility in remote rural areas where a significant amount of low-income population resides.

## 7. Implications and prospects

The estimated freshwater productivity rate is assumed to be the same throughout the entire lifetime of the solar still system. Although, some variation is to be expected due to fluctuation in the annual total solar irradiation and weather data pattern. Some of the cost estimates for materials correspond to the year of 2010, so adjusting for inflation with cost in 2021 terms, the median $LCOW$ is $\$8.36/m^3$ for the baseline case, and $\$2.04/m^3$ with the best case scenario. The increase in $LCOW$ is very small, and the freshwater cost is still within affordable limits (lower than 2.5% MHI) of the mentioned EPA guidelines. The cost associated with the brine intake is not considered due to inconsistencies in the literature, but this is expected to have less influence on the cost of water. Also, the treatment costs and brine disposal costs are considered from another published work on solar stills, but these vary based on location.

Next steps in this analysis include: (a) A more comprehensible model may be developed, (b) Elements such as indirect costs, operations, and maintenance costs used in this study were for large scale desalination systems. Specific values for small communities would provide a more accurate analysis, and (c) Freshwater produced by solar stills is usually considered to be free of salts as it was assumed in this manuscript. For actual utilization, appropriate experiments to determine toxic elements in the freshwater produced could be performed.

## 8. Conclusions

A solar still system utilizing low-cost black carbon particle dispersions as freshwater productivity enhancers was analyzed to determine the feasibility of meeting freshwater demand of small rural communities at affordable prices. From available candidate solar still materials, low-cost materials combinations were identified for to yield a low-cost solar still. With borosilicate glass as condensing cover, galvanized steel basin, rock wool insulation, concrete body, and silicone as sealant, the unit solar still cost is estimated to be only $32.5 per 1 $m^2$ of solar still basin area. Freshwater productivity in the reference region of California was determined using theoretical analysis and cost of freshwater production was computed using the $LCOW$ method. It was determined that the cost of freshwater produced in the reference state was almost uniform in the range between $\$6.36/m^3$ and $\$7.71/m^3$ with a median value of $\$6.89/m^3$. With some attractive investment options available, the cost of freshwater can be lower than $\$1.75/m^3$. For 20 identified low-income rural regions of California with fewer than 10 000 residents, the cost of freshwater produced is less than 1.5% of median household income. This is lower than the EPA recommended maximum freshwater affordability value of 2.5% of median household income. The freshwater produced is deemed feasible by comparing the freshwater production with competing mature technology like PV-RO, where the cost of freshwater produced was deemed higher than the solar stills. The reason is significantly low capital investment and maintenance cost of solar stills compared to PV-RO system. This methodology can be extrapolated and applied to other geographical locations to estimate feasibility of the solar still system the world to improve the access of freshwater in low-income rural communities.

## CRediT authorship contribution statement

**Sai Kiran Hota:** Writing – original draft, Techno-economic analysis. **Suryabhan Singh Hada:** Software, Computer Simulations. **Catherine Keske:** Economic Analysis, Reviewing, Editing. **Gerardo Diaz:** Advisor, Writing – review & editing.

## Declaration of competing interest

The authors declare that they have no known competing financial interests or personal relationships that could have appeared to influence the work reported in this paper.

## Data availability

Data will be made available on request.

## Acknowledgments

The authors wish to thank the California Energy Commission for partial funding of this study through grant #500-15-006. Also, the authors thank Mr. Anupam Misra, graduate student at UC Merced for helping with some of the simulations. We thank the Water & Energy Lab at UC Merced for providing computational resources.

## Appendix A. Supplementary data

Supplementary material related to this article can be found online at https://doi.org/10.1016/j.jclepro.2022.134595.

## References

Abdallah, S., Badran, O., Abu-Khader, M.M., 2008. Desalination 219 (1–3), 222–230.
Achari, G., Dore, M.H.I., Janzen, A., 2018. Int. J. Water Resour. Environ. Eng. 10 (6), 64–75. http://dx.doi.org/10.5897/IJWREE2018.0786.
Agarwal, A., Rana, R., Srivastava, P.K., 2017. Resour. Efficient Technol. 3, 466–482. http://dx.doi.org/10.1016/j.reffit.2017.05.003.
Al-Hinai, H., Al-Nassri, M.S., Jubran, B.A., 2002. Energy Convers. Manage. 43 (13), 1639–1650. http://dx.doi.org/10.1016/S0196-8904(01)00120-0.
Alwan, N.T., Shcheklein, S., Ali, O.M., 2021. Case Stud. Thermal Eng. 27, 101216.
Annibaldi, V., Cucchiella, F., Berardinis, P.D., Rotilio, M., Stornelli, V., 2019. Renew. Sustain. Energy Rev. 116, 109441. http://dx.doi.org/10.1016/j.rser.2019.109441.
Ashby, M.F., 2011. Materials Selection in Mechanical Design (Fourth Edition), Fourth Edition Butterworth-Heinemann, Oxford, pp. 495–523. http://dx.doi.org/10.1016/B978-1-85617-663-7.00018-7.
Bergman, T.L., Bergman, T.L., Incropera, F.P., Dewitt, D.P., Lavine, A.S., 2011. Fundamentals of heat and mass transfer. John Wiley & Sons.
Braulio-Gonzalo, M., Bovea, M.D., 2017. Energy Build. 150, 527–545. http://dx.doi.org/10.1016/j.enbuild.2017.06.005.
2019. Census reporter. URL: https://censusreporter.org/.
Chappelle, C., Collins, J., Hanak, E., 2022. Access to safe drinking water in california. URL: https://www.ppic.org/publication/access-to-safe-drinking-water.
Cooper, P., 1973. Solar Energy 15, 205–217. http://dx.doi.org/10.1016/0038-092X(73)90085-6.
Dsilva Winfred Rufuss, D., Raj Kumar, V., Suganthi, L., Iniyan, S., Davies, P., 2018. Sol. Energy 159, 820–833. http://dx.doi.org/10.1016/j.solener.2017.11.050.
Dunkle, R.V., 1961. A.S.M.E Proc. International Development in Heat Transfer, Vol. 5. pp. 895–902.
Durkaieswaran, P., Murugavel, K.K., 2015. Renew. Sustain. Energy Rev. 49, 1048–1060.
El-Dessouky, H.T., Ettouney, H.M., 2002. In: El-Dessouky, H.T., Ettouney, H.M. (Eds.), Fundamentals of Salt Water Desalination. Elsevier Science B.V., Amsterdam, pp. 503–524. http://dx.doi.org/10.1016/B978-044450810-2/50012-9.
Elango, C., Gunasekaran, N., Sampathkumar, K., 2015. Renew. Sustain. Energy Rev. 47, 856–911.
Feldman, D., Margolis, R., 2020. Q2/Q3 2020 Solar Industry Update. Technical Report, NREL.
Guo, J., Du, Z., Liu, G., Yang, X., Li, M.-J., 2022a. Appl. Thermal Eng. 206, 118124.
Guo, J., Liu, Z., Yang, B., Yang, X., Yan, J., 2022b. Renew. Energy 183, 406–422.
Guo, J., Wang, X., Yang, B., Yang, X., Li, M.-J., 2022c. Solar Energy Mater. Solar Cells 236, 111526.
Hill, C., Norton, A., Dibdiakova, J., 2018. Energy Build. 162, 12–20. http://dx.doi.org/10.1016/j.enbuild.2017.12.009.
2022. Homeadvisor. URL: https://www.homeadvisor.com/cost/foundations/concrete-footing/#footing-cost-calculator.
homewyse, 2020. Cost to excavate land. URL: https://www.homewyse.com/services/cost_to_excavate_land.html.
Hoque, A., Abir, A.H., Shourov, K.P., 2019. Appl. Water Sci. 9 (104), http://dx.doi.org/10.1007/s13201-019-0986-9.
Hota, S.K., Diaz, G., 2019. Sol. Energy 184, 40–51. http://dx.doi.org/10.1016/j.solener.2019.03.080.
Hota, S.K., Diaz, G., 2021. Environ. Eng. Sci. 38 (12), 1120–1128.
Hota, S.K., Duong, V., Diaz, G., 2020. Heat Mass Transf. 56, 109–120. http://dx.doi.org/10.1007/s00231-019-02686-y.
Hota, S.K., Mata-Torres, C., Cardemil, J.M., Diaz, G., 2022. Desalin. Water Treat. 245, 72–84. http://dx.doi.org/10.5004/dwt.2022.27942.
Hota, S.K., Perez, J., Diaz, G., 2018. ASME 2018 International Mechanical Engineering Congress and Exposition. American Society of Mechanical Engineers Digital Collection, pp. IMECE2018–87852: 1–7.
Howe, E.D., Tleimat, B.W., 1974. Sol. Energy 16 (2), 97–105. http://dx.doi.org/10.1016/0038-092X(74)90005-X.
Jahanpanah, M., Sadatinejad, S.J., Kasaeian, A., Jahangir, M.H., Sarrafha, H., 2021. Desalination 499, 114799.
Jones, P.A., Moulton, A., 2016. The invisible crisis: Water unaffordability in the United States. Unitarian Universalist Service Committee.
Kalogirou, S.A., 2005. Prog. Energy Combust. Sci. 31 (3), 242–281. http://dx.doi.org/10.1016/j.pecs.2005.03.001.
Kecebas, A., Kayveci, M., 2010. Energy Educ. Sci. Technol. Part A 25, 117–127.
Kumar, D., Zou, P.X.W., Memon, R.A., Alam, M.M., Sanjayan, J.G., Kumar, S., 2020. J. Build. Phys. 43 (5), 428–455. http://dx.doi.org/10.1177/1744259119857749.
Kunič, R., 2017. Energy Efficiency 10, 1511–1528. http://dx.doi.org/10.1007/s12053-017-9536-1.
Lawrence, S.A., Gupta, S.P., Tiwari, G.N., 1988. Int. J. Sol. Energy 6 (5), 291–305. http://dx.doi.org/10.1080/01425918808914235.
MacDonald, G.M., 2007. Quat. Int. 173–174, 87–100. http://dx.doi.org/10.1016/j.quaint.2007.03.012.
Mack, E.A., Wrase, S., 2017. PLoS One 12 (1), e0169488.
Madani, A.A., Zaki, G.M., 1995. Appl. Energy 52 (2), 273–281. http://dx.doi.org/10.1016/0306-2619(95)00044-S, Fifth Arab International Solar Energy Conference.
Malek, A., Hawlader, M.N.A., Ho, J.C., 1996. Desalination 105 (3), 245–261. http://dx.doi.org/10.1016/0011-9164(96)00081-1.
Masters, G.M., 2013. Renewable and Efficient Electric Power Systems. Wiley-IEEE Press, pp. 629–644.
Mathioulakis, E., Belessiotis, V., Delyannis, E., 2007. Desalination 203 (1–3), 346–365.
Meratizaman, M., Monadizadeh, S., Tohidi Sardasht, M., Amidpour, M., 2015. Energy 83, 1–14. http://dx.doi.org/10.1016/j.energy.2015.01.112.
Modest, M.F., Mazumder, S., 2021. Radiative Heat Transfer. Academic Press.
Murugavel, K.K., Sivakumar, S., Ahamed, J.R., Chockalingam, K.K., Srithar, K., 2010. Appl. Energy 87 (2), 514–523.
National tank outlet, 2003. Underground water cistern tanks. URL: https://www.ntotank.com/underground-water-tanks.
Parkin, R.E., 2015. Sol. Energy 114, 196–197. http://dx.doi.org/10.1016/j.solener.2015.01.004.
SAER-USA, 2020a. SAER heavy duty centrifugal water pump. URL: www.pumpsupermarket.com/product/saer-usa-6bp7-109-1ph-threaded-centrifugal-pump-19200-gph-3-hp-3in-ports-230-volts/.
SAER-USA, 2020b. SAER heavy duty centrifugal water pump. URL: www.pumpsupermarket.com/product/saer-usa-6bp4-110-threaded-centrifugal-pump-9480-gph-1-5-hp-2in-ports/.
Schiavoni, S., D'Alessandro, F., Bianchi, F., Asdrubali, F., 2016. Renew. Sustain. Energy Rev. 62, 988–1011. http://dx.doi.org/10.1016/j.rser.2016.05.045.
Sengupta, M., Xie, Y., Lopez, A., Habte, A., Maclaurin, G., Shelby, J., 2018. Renew. Sustain. Energy Rev. 89, 51–60. http://dx.doi.org/10.1016/j.rser.2018.03.003.
State of Michigan, 2003. Tanks section UIP 11. URL: https://www.michigan.gov/documents/Vol2-35UIP11Tanks_121080_7.pdf.
Thomas, K.E., 1997. Overview of village scale, renewable energy powered desalination. Technical Report NREL/TP-440-22083, National Renewable Energy Laboratory, http://dx.doi.org/10.2172/463614.
Tiwari, G., Shukla, S., Singh, I., 2003. Desalination 154 (2), 171–185. http://dx.doi.org/10.1016/S0011-9164(03)80018-8.
United States Plastic Corp, 2020. HI-temp CPVC pipe schedule 40 & 80. URL: https://www.usplastic.com/catalog/item.aspx?itemid=23484&catid=521.
2019. U.S. census buraeu. URL: https://www.census.gov/quickfacts/fact/table/CA/PST045219.
Velmurugan, V., Gopalakrishnan, M., Raghu, R., Srithar, K., 2008. Energy Convers. Manage. 49 (10), 2602–2608.
Vogt, M.R., Hahn, H., Holst, H., Winter, M., Schinke, C., Kantges, M., Brendel, R., Altermatt, P.P., 2016. IEEE J. Photovolt. 6 (1), 111–118. http://dx.doi.org/10.1109/JPHOTOV.2015.2498043.
Walther, A., Heidinger, A.K., 2012. J. Appl. Meteorol. Climatol. 51 (7), 1371–1390. http://dx.doi.org/10.1175/JAMC-D-11-0108.1.
2007. Water systems council. URL: https://www.watersystemscouncil.org/download/wellcare_information_sheets/potential_groundwater_contaminant_information_sheets/2010920TDS_FINAL.pdf.
Yang, X., Guo, J., Yang, B., Cheng, H., Wei, P., He, Y.-L., 2020. Appl. Energy 279, 115772.
Yang, X., Wang, X., Liu, Z., Luo, X., Yan, J., 2022. Solar Energy Mater. Solar Cells 236, 111527.
Zheng, H., 2017. In: Zheng, H. (Ed.), Solar Energy Desalination Technology. Elsevier, Amsterdam, pp. 259–321. http://dx.doi.org/10.1016/B978-0-12-805411-6.00004-X.
Ziolkowska, J., Reyes, R., 2017. In: Ziolkowska, J.R., Peterson, J.M. (Eds.), Competition for Water Resources. Elsevier, pp. 298–316. http://dx.doi.org/10.1016/B978-0-12-803237-4.00017-3.
Zoori, H.A., Tabrizi, F.F., Sarhaddi, F., Heshmatnezhad, F., 2013. Desalination 325, 113–121.